JOURNAL OF VIROLOGY, Jan. 2011, p. 334–347 Vol. 85, No. 1
0022-538X/11/$12.00 doi:10.1128/JVI.01278-09

The Tyro3 Receptor Kinase Axl Enhances Macropinocytosis of Zaire Ebolavirus▽

Catherine L. Hunt,[1] Andrey A. Kolokoltsov,[2] Robert A. Davey,[2] and Wendy Maury[1]*

Department of Microbiology, University of Iowa, Iowa City, Iowa,[1] and Department of Microbiology and Immunology, Galveston National Laboratory, University of Texas Medical Branch, Galveston, Texas[2]

Received 22 June 2009/Accepted 20 October 2010

Axl, a plasma membrane-associated Tyro3/Axl/Mer (TAM) family member, is necessary for optimal Zaire ebolavirus (ZEBOV) glycoprotein (GP)-dependent entry into some permissive cells but not others. To date, the role of Axl in virion entry is unknown. The focus of this study was to characterize entry pathways that are used for ZEBOV uptake in cells that require Axl for optimal transduction and to define the role of Axl in this process. Through the use of biochemical inhibitors, interfering RNA (RNAi), and dominant negative constructs, we demonstrate that ZEBOV-GP-dependent entry into these cells occurs through multiple uptake pathways, including both clathrin-dependent and caveola/lipid raft-mediated endocytosis. Other dynamin-dependent and -independent pathways such as macropinocytosis that mediate high-molecular-weight dextran uptake also stimulated ZEBOV-GP entry into these cells, and inhibitors that are known to block macropinocytosis inhibited both dextran uptake and ZEBOV infection. These findings provided strong evidence for the importance of this pathway in filovirus entry. Reduction of Axl expression by RNAi treatment resulted in decreased ZEBOV entry via macropinocytosis but had no effect on the clathrin-dependent or caveola/lipid raft-mediated endocytic mechanisms. Our findings demonstrate for the first time that Axl enhances macropinocytosis, thereby increasing productive ZEBOV entry.

Filoviruses are enveloped, nonsegmented, negative-stranded RNA viruses capable of causing severe hemorrhagic fever in humans, nonhuman primates, and other mammals, resulting in high rates of death associated with infection. African fruit bats such as *Rousettus aegyptiacus* are believed to serve as a reservoir for filoviruses in the wild (12, 30, 31, 43, 45, 46, 55, 70, 72–74). Filoviruses have a very broad cellular and species tropism, mediating entry into almost all avian and mammalian cells (19, 69, 71, 79, 80). Some cells are more permissive to filovirus entry than others. For instance, lymphocytes are poorly permissive for filovirus infection whereas endothelial cells, fibroblastic cells, macrophages, and epithelial cells are, in general, highly permissive. *In vivo*, filoviruses infect most major organ systems, including the liver, kidney, spleen, adrenal gland, and brain in humans, mice, guinea pigs, and nonhuman primates (8, 15, 25, 28). The wide tropism exhibited by the filoviruses results from the ability of the filoviral glycoprotein (GP) to mediate entry into many different cell types.

The filoviruses are pathogens that require biosafety level 4 (BSL-4) conditions. Thus, investigators have turned to pseudotyping the filovirus glycoproteins onto noninfectious lentivirions or rhabdovirions. Recent studies with ebolavirus (EBOV)- or Lake Victoria marburgvirus (MARV)-GP pseudovirions have provided significant insights into steps involved with productive cellular entry of this deadly pathogen (9, 13, 42, 49, 52, 61–63, 76, 81).

To enter cells, EBOV must bind to target cells and internalize into endocytic vesicles (13, 19, 59, 61, 79). Within the endosome, low-pH-dependent proteolysis of the viral surface GP (GP1) is required for GP2-dependent fusion of the virus with cellular membranes (13, 61). The mechanism(s) that mediates filovirus uptake into the endosomal compartment remains controversial. Early reports indicated that the caveola vesicular system and/or lipid raft domains were important for EBOV-GP-mediated entry (4, 22, 81). However, another study demonstrated that overexpression of caveolin 1 (Cav1) in the poorly permissive lymphocytic cell line CEM did not enhance levels of EBOV-GP-dependent transduction, suggesting that caveolae may not play a role in filovirus entry (66). In 2007, Sanchez reported in a preliminary study that infectious EBOV enters endosomes through a variety of different uptake mechanisms, including caveolae and clathrin-coated pits, and through actin- and microtubule-dependent pathways in VeroE6 cells (59). A recent study confirmed that clathrin-coated pits are indeed utilized by infectious EBOV to enter permissive cells (6). It has also been speculated that, because of their large size, filoviruses may utilize macropinocytosis to enter permissive cells (19, 56). Recently, the latter mechanism of entry was demonstrated experimentally for the first time for a filovirus (51, 57).

While the receptor(s) that interacts with filovirus glycoprotein and mediates virus entry into cells remains to be identified, several proteins have been shown to enhance filoviral entry into cells. One of these proteins is the Tyro3 receptor kinase family member Axl. Axl enhances filoviral transduction of some highly permissive cells such as HeLa cells but not others such as Vero and VeroE6 cells. Although it appears that the Axl ectodomain and filoviral GPs do not directly interact, Axl expression increases virus internalization and subsequent membrane fusion (M. A. Brindley, C. L. Hunt, A. S. Kondratowicz, J. Bowman, P. L. Sinn, P. B. McCray, Jr., K. Quinn,

* Corresponding author. Mailing address: 3-750 Bowen Science Bldg, Dept. Microbiology, University of Iowa, Iowa City, IA 52242. Phone: (319) 335-8021. Fax: (319) 335-9006. E-mail: wendy-maury@uiowa.edu.

▽ Published ahead of print on 3 November 2010.

M. L. Weller, J. A. Chiorini, and W. Maury, submitted for publication). In total, the findings suggest that Axl is not a receptor for the filoviruses but is responsible for somehow facilitating filovirus uptake. This study was undertaken to determine if Axl alters mechanisms of endocytic uptake of filoviruses. Indeed, we found that Axl expression enhanced filovirus uptake through stimulation of macropinocytosis in Axl-dependent cells.

MATERIALS AND METHODS

Cell lines and antibodies. Human embryonic kidney cell line 293T (CRL-11268; ATCC); a human glioblastoma line, SNB19 (NCI 0502596); and an African green monkey kidney cell line, Vero (CCL-81; ATCC), were maintained in high-glucose Dulbecco's modified Eagle's medium (DMEM) (Invitrogen) supplemented with 1% penicillin and streptomycin (P/S) and 10% fetal calf serum (FBS) (HyClone). Cells were maintained at 37°C with 5% CO_2. Primary human foreskin fibroblasts (Hffs) isolated from fresh penile foreskin were maintained in DMEM supplemented with 1% P/S and 15% FBS. Primary human umbilical vein macrovascular endothelial cells (HuVECs) isolated from a fresh umbilical cord were maintained in endothelial cell basal medium (EBM) supplemented with bovine brain extract, human epidermal growth factor (hEGF), hydrocortisone, gentamicin, amphotericin B, and 5% fetal calf serum (Lonza/Cambrex). Antibodies used included anti-human Axl (R&D Systems), anti-human caveolin 1 (Cav1) (AbCam), anti-human caveolin 2 (Cav2) (BD Biosciences), and anti-human actin (AbCam).

Plasmids used. Plasmids used to generate the feline immunodeficiency virus (FIV)-ZEBOVΔO and FIV-vesicular stomatitis virus (VSV) G (Indiana strain) particles have been previously described (37, 68, 75). Wild-type Eps15 (wtEps15) and dominant negative Eps15 (DNEps15) expression plasmids have been previously used to specifically disrupt clathrin-mediated endocytosis (10). The plasmid bearing ZEBOV matrix protein (VP40) (Entrez gene NC002549) was kindly provided by Ronald Harty (University of Pennsylvania). The plasmid bearing the firefly luciferase gene driven by the Rous sarcoma virus promoter (67) has been previously described. Plasmids bearing the full-length ZEBOV-GP (37) and the full-length Lake Victoria MARV-GP (Musoke variant) (78) have also been described previously.

Generation and detection of pseudovirions and virus-like particles (VLPs). FIV pseudovirions were generated in 293T cells as previously described (9, 68, 75). All pseudovirions were concentrated using a 16-hour centrifugation step at 7,000 rpm at 4°C in a Sorvall GSA rotor. The viral pellet was resuspended in 250 μl DMEM for an approximately 200-fold concentration prior to use. All FIV pseudovirions expressed the reporter β-galactosidase (β-Gal) upon delivery into the recipient cell. FIV transduction studies were performed in a 48-well format using a multiplicity of infection (MOI) of ~0.005 (resulting in approximately 200 β-Gal-positive cells/40,000 cells/well in control wells). FIV pseudovirion transduction was detected by fixing cells in 3.7% formalin and evaluating them for β-Gal activity by using the substrate 5-bromo-4-chloro-3-indolyl-β-D-galactopyranoside. All FIV transduction evaluation was done 48 h after initial FIV pseudovirion addition to cells. β-Gal-positive cells were enumerated by microscopic visual inspection.

VSVΔG/enhanced green fluorescent protein (eGFP) pseudovirions (a kind gift of Michael Whitt, University of Tennessee Health Sciences) bearing full-length ZEBOV-GP (VSVΔG-ZEBOV-FL) or Lake Victoria MARV-GP (VSVΔG-MARV) were generated in 293T cells as previously described (56). For detection of VSVΔG/eGFP pseudovirion transduction, 24 h following transduction, cells were lifted in Accumax (Fisher) and analyzed with a FACScan cytometer (BD Biosciences) for FL-1 intensity. VSVΔG pseudovirions were applied to cells to yield approximately 1,000 GFP-positive cells for every 20,000 cells analyzed by flow cytometry. This gives an MOI of approximately 0.05 for all studies using the VSVΔG system.

ZEBOV-VLPs were generated in 293T cells by transfection of 75 μg total of a 1:1:1 ratio of ZEBOVΔO-GP, ZEBOV VP40, and firefly luciferase-bearing plasmids by using a standard calcium phosphate transfection protocol. The luciferase protein expressed in the transfected cell was nonspecifically incorporated into VLPs. VLPs in the cell supernatant were collected every 12 h from 36 to 72 h. VLPs were concentrated using a 16-hour centrifugation step at 7,000 rpm at 4°C in a Sorvall GSA rotor. The VLP pellet was resuspended in 250 μl DMEM for an approximately 200-fold concentration prior to use. Equivalent amounts of VLPs were added to all virus-treated cells in each experiment. Seven hours following infection, cells were washed to remove unbound particles, lysed in equal parts sterile phosphate-buffered saline (PBS) and SteadyGlo (Promega), and assayed for luminescence per the manufacturer's protocol.

Because there is some variation in absolute numbers of on-put virions used between different experiments and all experiments shown are a compilation of at least three different experiments, the control findings were set to 100% and the results shown are represented as percentages of control values rather than absolute transduction values.

RNAi. SNB19 cells or Hffs (0.75×10^6) were transfected with 200 pmol of a mixture of small interfering RNAs (siRNAs) against Cav1 (Invitrogen catalog no. 15299372) or Cav2 (Invitrogen catalog no. 16495103) in a 6-well format. SNB19 or Hff cells (2×10^6) were transfected with 500 pmol of human Axl (two Axl-validated interfering RNA [RNAi] constructs; Invitrogen) in a T25 tissue culture flask. Appropriate concentrations of control fluorescently labeled nonspecific siRNA (Block-It; Invitrogen) or RNAi against luciferase were transfected as a control. All transfections were performed using the Lipofectamine 2000 (Invitrogen) protocol. Transfected cell populations were plated in a 48-well format at 24 h post-RNAi transfection. At 48 h following transfection, cells were transduced with FIV pseudovirions in the presence or absence of macropinocytosis inhibitors, used for dextran uptake studies, or harvested for immunoblotting analysis.

Infectious ZEBOV studies. Twenty-four hours after siRNA transfection, cells were split into a 96-well plate at a concentration of 10^4 cells per well. Twenty-four hours later, cells were pretreated with 5-(*N*-ethyl-*N*-isopropyl)amiloride (EIPA), cytochalasin B (CYTO-B), or dimethyl sulfoxide (DMSO) control at indicated concentrations. After 1 h, Zaire ebolavirus encoding GFP (kind gift of J. Towner, CDC) was added to cells at an MOI of 0.25. At 18 h, the culture medium was replaced with fresh medium without drugs. After an additional 6 h, the medium was removed and cells were fixed in formalin for 48 h. Infected cells were then analyzed for GFP positivity (compared to number of cell nuclei stained with 4′,6-diamidino-2-phenylindole [DAPI]) to generate a "proportion of infected cells" calculation. All experiments with ZEBOV were performed under biosafety level 4 conditions in the Robert E. Shope BSL-4 Laboratory, University of Texas Medical Branch (UTMB).

Cell transfection with Eps15 constructs. SNB19 cells (10^6) were transfected with 5 μg of either wtEps15 or DNEps15 expression plasmids by using 100 μl Amaxa solution T and program L-029 with the Amaxa nucleotransfection device. Transfected cells were distributed into 24 wells of a 48-well plate. Cells were transduced with FIV pseudovirions 24 h after plasmid transfection.

Ad DN dynamin studies. SNB19 cells, Hffs, or HuVECs (4×10^4) were plated in a 48-well format. Adenovirus (Ad) vectors expressing GFP or DN dynamin 2 (DNdyn2) (K44A) (a gift from Jeff Pessin, SUNY-Stony Brook) were incubated with the cells for 24 h (41). Ad vector transduction efficiency was determined by the percentage of cells expressing GFP, which was greater than 95%. Cells were transduced with FIV pseudovirions 24 h after Ad transduction.

Drug studies. All chemical reagents were obtained from Sigma (St. Louis, MO) unless noted. All studies were performed in a 48-well format on 4×10^4 cells per well. Concentrations of drugs are noted in figures. The no-drug control contained the appropriate dilution of vehicle. Cells were preincubated with drug for 1 h before the addition of pseudovirions. The drug remained on the cells for an additional 6 h during the transduction (except for filipin [FIL]). FIL-containing medium (serum free) was removed before virions were added in fresh medium without serum. Transduced cells were assessed for β-Gal activity 48 h after the initial addition of pseudovirions (FIV system) or 24 h after the initial addition of pseudovirions (VSVΔG system). The findings are shown as the ratio of the number of transduced cells in the presence of inhibitor divided by the number of transduced cells when no inhibitor was added (percentage of control). In all inhibitor studies, the ability of the inhibitors to decrease pseudovirion transduction was adjusted for cytotoxicity associated with the inhibitor.

CPZ. Chlorpromazine (CPZ) was resuspended in ethanol at 1 mg/ml. CPZ was diluted into the medium (containing FBS) and preincubated with cells for 1 h. Cells were transduced in the presence of the drug, and the CPZ-containing inoculum was removed 6 h after transduction and replaced with fresh, chlorpromazine-free medium (DMEM containing 10% FBS and 1% P/S).

FIL. Filipin (FIL) was resuspended in methanol at 5 mg/ml. Filipin was diluted into DMEM (without FBS) and preincubated with cells for 1 h. The filipin-containing medium was removed and replaced with fresh medium (without FBS or filipin) containing FIV pseudovirions. The medium was then refreshed with medium 24 h after the initial addition of pseudovirions.

BLB. Blebbistatin (BLB) was resuspended in DMSO at 100 mM. BLB was diluted into the medium (containing FBS) and preincubated with cells for 1 h. Cells were transduced in the presence of the drug, and the blebbistatin-containing inoculum was removed 5 h after FIV pseudovirion transduction and replaced with fresh medium that did not contain inhibitor.

EIPA. 5-(*N*-Ethyl-*N*-isopropyl)amiloride (EIPA) was resuspended in dimethyl sulfoxide (DMSO) at 200 mM. EIPA was diluted into the medium (containing FBS) and preincubated with cells for 1 h. Cells were transduced in the presence of the drug, and the EIPA-containing inoculum was removed 5 h after FIV pseudovirion transduction and refreshed with fresh medium not containing inhibitor.

CYTO-B. Cytochalasin B (CYTO-B) was obtained from Calbiochem and was resuspended in DMSO at 25 mM. CYTO-B was diluted in medium and incubated with cells for 1 h. Cells were transduced in the presence of the drug, and the drug-containing inoculum was removed 5 h after FIV pseudovirion transduction and refreshed with medium not containing inhibitor.

Dynasore. Dynasore was resuspended at 100 mM in DMSO. The drug was diluted in medium and incubated with cells for 1 h. Cells were transduced in the presence of the drug, and the drug-containing inoculum was removed 5 h after FIV pseudovirion transduction and refreshed with medium not containing inhibitor.

Detection and analysis of labeled conjugate uptake. All conjugates were purchased from Invitrogen. Dextran (70 kDa, conjugated to fluorescein isothiocyanate [FITC]) was resuspended in sterile H_2O at 10 mg/ml. Human transferrin (Tfr) and cholera toxin subunit B (CTb) conjugated to Alexa Fluor 647 were resuspended in sterile H_2O at a concentration of 5 mg/ml and 1 mg/ml, respectively. For drug studies with dextran, Tfr, or CTb, cells were pretreated with drug alone for 1 h followed by addition of the labeled conjugate for an additional hour in the presence of drug. Cells were washed three times in sterile PBS and lifted with Accumax (Fisher) for analysis of the geometric mean of intensity by flow cytometry on a FACScan cytometer (BD Biosciences) using FL-1 (dextran) or FL-4 (Tfr and CTb) channels. The geometric mean of the control cell population was divided by the geometric mean of the drug-treated cell population and multiplied by 100% to yield a "percent control" value.

Immunoblotting. Cells were lysed, and proteins were separated using SDS-PAGE as described previously (9). Cav1, Cav2, and Axl were detected by incubation with primary antibodies (1:1,000, 1:250, and 1:4,000 dilutions, respectively) overnight at 4°C followed by incubation with appropriate secondary peroxidase-conjugated antisera (1:20,000; Sigma). Actin was detected by incubating primary peroxidase-conjugated antibody (1:10,000) for 3 h at room temperature. Membranes were visualized by the chemiluminescence method according to the manufacturer's protocol (Pierce).

Confocal microscopy. SNB19 cells (3.5×10^4 cells) were plated on collagen-coated coverslips and incubated overnight at 37°C to allow cells to adhere. Cells were then incubated with FIV-ZEBOVΔO pseudovirions (MOI, 250) at 4°C for 1 h. Nonbound virus was removed, cells were washed once in 1× PBS, and cells were shifted to 37°C. At the indicated time, cells were fixed in 2% paraformaldehyde and permeabilized with 0.2% Triton X-100. Virus (green) was detected with anti-FIV monoclonal antibody (1:50; NIH AIDS Research and Reference Reagent Program catalog no. 4816) and Alexa Fluor 488 chicken anti-mouse antibody (1:200; Invitrogen). Polymerized actin (blue) was detected with Alexa Fluor 647 phalloidin (1:200; Invitrogen). Microscopy was performed on a Nikon Eclipse 80i confocal microscope.

Cell viability assay. At the time of pseudovirion transduction evaluation, cell viability was monitored in an ATP-Lite assay (Packard Biosciences) per the manufacturer's instructions.

Statistical analysis. Statistical analyses were conducted by Student's *t* test, utilizing the two-tailed distribution and two-sample equal-variance conditions. *P* values were assessed by comparing the level of transduction with treatment to the level of cytotoxicity observed with that specific treatment. A significant difference was determined by a *P* value of <0.05. If the *P* value was >0.05, the data were not considered significant.

RESULTS

Axl is required for efficient Zaire ebolavirus (ZEBOV) infection and ZEBOV-GP-dependent pseudovirion transduction into some cells. Earlier studies have shown that ectopic expression of Axl in HEK 293T cells increases ZEBOV pseudovirion transduction but only modestly increases ZEBOV infection (63). We sought to assess the requirement of Axl expression for ZEBOV infection in cells that endogenously express Axl by using a neuroblastoma cell line, SNB19, as a model cell system for our studies. SNB19 cells express large quantities of Axl on their cell surface and have proved to be one of the most highly ZEBOV-GP pseudovirion-transducible lines from a large panel of well-characterized human tumor lines, NCI-60 (Brindley et al., submitted). Additionally, the cells were readily transfectable.

To evaluate the effect of Axl on ZEBOV infection of these cells, SNB19 cells were transfected with 200 pmol of nonspecific RNAi or RNAi specific for Axl. Transfected cell lysates were immunoblotted for Axl, and efficient knockdown of Axl by Axl RNAi, but not by an irrelevant RNAi, was evident (Fig. 1B). At 48 h following transfection, these RNAi-transfected cells were infected with ZEBOV that expresses eGFP (Fig. 1A). A reduction of Axl expression decreased ZEBOV infectivity by ~80%, demonstrating for the first time the importance of endogenous Axl expression for filovirus infection. We termed cells, such as SNB19 cells, that require Axl for optimal ZEBOV infection Axl-dependent cells. RNAi knockdown of Axl also decreased transduction of a mucin domain-deleted ZEBOV-GP (ZEBOVΔO)-pseudotyped FIV (FIV-ZEBOVΔO) (Fig. 1C and D). As ZEBOVΔO-GP has been shown to have the same cell tropism as that of wild-type ZEBOV-GP with higher viral titers (37), we used this filovirus glycoprotein in many of these studies. However, to further validate our ZEBOV pseudovirion transduction system, we tested the ability of polyclonal antisera against the Axl ectodomain to block entry of full-length ZEBOV-GP and MARV-GP pseudotyped onto a different pseudovirion, vesicular stomatitis virus, producing VSVΔG-ZEBOV-FL or VSVΔG-MARV pseudovirions. The Axl antiserum was able to significantly reduce transduction of these viral particles into SNB19 cells (Fig. 1E) as well as VSV-ZEBOVΔO entry in HeLa cells (data not shown), a cell line previously shown to require Axl for optimal filoviral transduction (63). These findings with our pseudovirions indicate that our FIV-ZEBOV transduction studies can serve to model ZEBOV infection mechanisms in a BSL-2 setting, allowing us to assess the role of Axl in filovirus entry.

Clathrin-mediated endocytosis is utilized by FIV-ZEBOVΔO for entry into Axl-dependent cells. To date, endocytic mechanisms used during ZEBOV entry have been investigated only in cells such as Vero, HEK 293T, or VeroE6 cells that do not require Axl expression for filovirus infection, which we call Axl-independent cells (6, 22, 59, 81); similar studies in Axl-dependent cells have not been performed. To determine if clathrin-coated pits mediated ZEBOV-GP-dependent entry into cells that require Axl expression for optimal ZEBOV infection, SNB19 cells were treated with increasing concentrations of chlorpromazine (CPZ). CPZ has been used extensively to evaluate the role of clathrin-coated pits as it prevents clathrin-mediated endocytosis by redirecting clathrin adaptor proteins from plasma membrane proteins to internal membranes (36). Drug-treated and untreated cells were transduced with FIV-ZEBOVΔO. The effect of CPZ (and all treatments used in these studies) on cell viability was evaluated in parallel. FIV-ZEBOVΔO transduction was inhibited in a dose-dependent manner by CPZ with little detectable toxicity in SNB19 cells (Fig. 2A). We confirmed the effect of CPZ on ZEBOV transduction in Axl-expressing primary human foreskin fibroblasts (Hffs), as fibroblasts have been shown to be important for ZEBOV replication *in vivo* (Fig. 2C) (15, 17, 24). In other studies, we have also demonstrated that optimal transduction of ZEBOV pseudovirions into Hffs and another primary cell

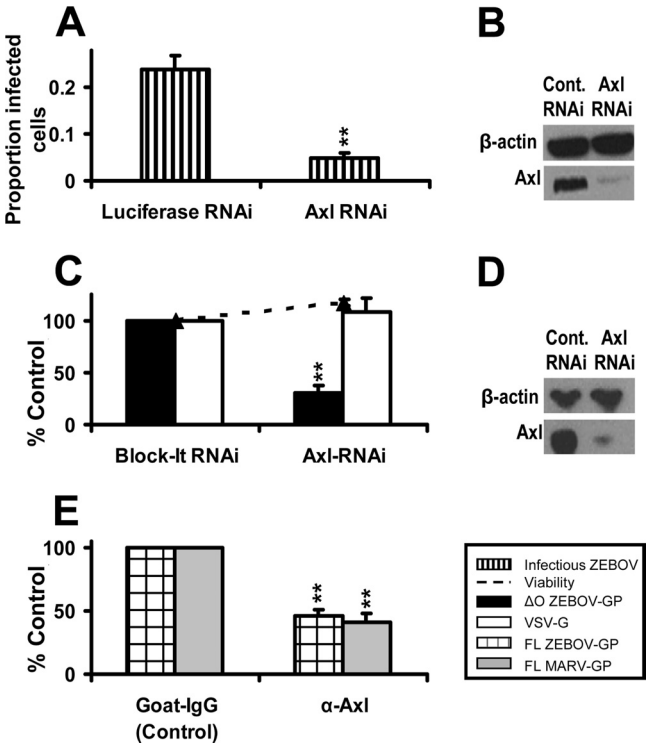

FIG. 1. Axl is necessary for efficient infectious Zaire ebolavirus infection and FIV-ZEBOV transduction into Axl-dependent cells. (A and C) Effect of Axl RNAi on ZEBOV infection or transduction. SNB19 cells were transfected with 200 pmol of a nonspecific luciferase siRNA control (A), 200 pmol of a nonspecific siRNA control (Block-It) (C), or 200 pmol of a human Axl-specific siRNA (A and C). At 48 h following RNAi transfection, cells were infected with ZEBOV (A) (MOI, 0.25) for 24 h or transduced with FIV pseudovirions for 48 h (C) (MOI, 0.005). At 24 h following infection, cells were fixed and analyzed by microscopy for GFP positivity relative to the number of cells for each condition (A), or at 48 h following transduction, cells were fixed and stained for β-Gal activity (C). (B and D) Knockdown of Axl by RNAi. At 48 h after RNAi transfection, a portion of the transfected cells were lysed, proteins were separated using SDS-PAGE, and Axl was detected on the nitrocellulose membrane with primary antiserum (1:4,000) overnight at 4°C. The signal was detected by incubation with secondary horseradish peroxidase-conjugated antiserum (1:20,000) for 1 h at room temperature followed by visualization by chemiluminescence. Actin was detected by incubation with horseradish peroxidase-conjugated anti-actin antibody. The immunoblots shown are representative of three experiments performed independently. (E) Ability of Axl antiserum to block transduction of FIV-ZEBOV or FIV-MARV. A 1:50 dilution of goat anti-human Axl antiserum or normal goat serum was incubated with SNB19 cells for 1 h at 4°C. VSVΔG pseudovirions (MOI, 0.05) bearing full-length ZEBOV-GP or MARV-GP were applied in the presence of antiserum and incubated for an additional 23 h. Cells were lifted and analyzed by flow cytometry for GFP positivity, indicating viral transduction. Data represent the averages and standard errors of three experiments performed in triplicate. **, $P < 0.001$.

population, human umbilical cord endothelial cells (HuVECs), requires Axl expression (Brindley et al., submitted).

Vesicular stomatitis virus G glycoprotein (VSV-G)-dependent transduction was used as a positive control for the CPZ studies because VSV-G entry into other cell lines has been reported to be clathrin dependent (16, 39). As expected, FIV-VSV-G was inhibited by 5 μg/ml of CPZ. The impact of CPZ on uptake of fluorescent transferrin (Tfr) and cholera toxin subunit B (CTb) was also evaluated in SNB19 cells, as Tfr is a marker of uptake via clathrin-coated pits (20), whereas CTb is a marker of uptake via caveolin/lipid raft-mediated endocytosis (18). As expected, CPZ did not affect uptake of CTb but decreased uptake of Tfr, indicating that CPZ was indeed affecting clathrin-mediated endocytic events (Fig. 2A). These studies indicated that clathrin-dependent mechanisms are important for ZEBOV-GP-mediated entry into Axl-dependent SNB19 and Hff cells.

The biochemical finding that ZEBOV-GP-dependent transduction was blocked by inhibition of clathrin-coated pit formation was independently verified via ectopic expression of the dominant negative (DN) form of the clathrin-associated protein Eps15. Eps15 serves as a protein bridge between the cargo being internalized and the clathrin coat (18). pDN-Eps15Δ95-295-GFP (DNEps15) inhibits clathrin-mediated uptake because it lacks the Eps homology domains necessary for clathrin-coated pit targeting, whereas pEps15Δ5Δ2-GFP expresses wild-type Eps15 (wtEps15) (10). SNB19 cells transfected with the Eps constructs were transduced 24 h later with either FIV-ZEBOVΔO or FIV-VSV-G. Transduction of both pseudovirions was decreased by 40 to 60% in cells expressing the DNEps15 construct but not in cells expressing wtEps15 (Fig. 2B). SNB19 cells expressing the DNEps15 construct also showed a significantly decreased ability to take up Tfr, but not CTb, indicating that the expression of DNEps15 was specifically inhibiting clathrin-mediated endocytosis in these cells. These results support our findings with CPZ that ZEBOV-GP-dependent entry utilizes clathrin-mediated endocytosis as a mechanism of entry into SNB19 cells.

Cholesterol is important for efficient ZEBOV-GP pseudovirion entry into Axl-dependent cells. Cholesterol is a principal component of plasma membrane lipid rafts (34). While lipid raft-associated endocytosis has been primarily linked to caveola-dependent uptake (34), recent studies have found that clathrin-dependent endocytosis and macropinocytosis can also be associated with lipid rafts (19, 77). To determine the role of host plasma membrane cholesterol in ZEBOV-GP-mediated entry, cells were treated with the drug filipin (FIL) to bind to cholesterol and disrupt lipid rafts (53). FIL treatment did not inhibit the entry of FIV-VSV-G (Fig. 2D) but decreased transduction of FIV-ZEBOVΔO into SNB19 cells by ~40% (Fig. 2D). A similar trend was observed in Hffs (data not shown). Additionally, FIL inhibited about 40% of CTb uptake but not Tfr uptake in SNB19 cells, indicating that the FIL drug was specifically acting on an endocytic pathway involving membrane cholesterol and lipid rafts and was not affecting clathrin-coated pit formation in these cells (Fig. 2D). Our findings are consistent with previously published results demonstrating that ZEBOV-GP-dependent entry is blocked by treatment of SNB19 cells with the cholesterol-sequestering drug methyl-beta-cyclodextrin (10) and indicate that plasma membrane cholesterol and lipid rafts are important for efficient ZEBOV-GP-mediated entry into these cells.

Caveolin is involved in ZEBOV-GP pseudovirion entry into Axl-dependent cells. The inhibition of ZEBOV-GP-mediated entry by loss of plasma membrane cholesterol suggested that caveolae might be involved in ZEBOV-GP-dependent entry into Axl-dependent cells. Caveola dependence of ZEBOV-

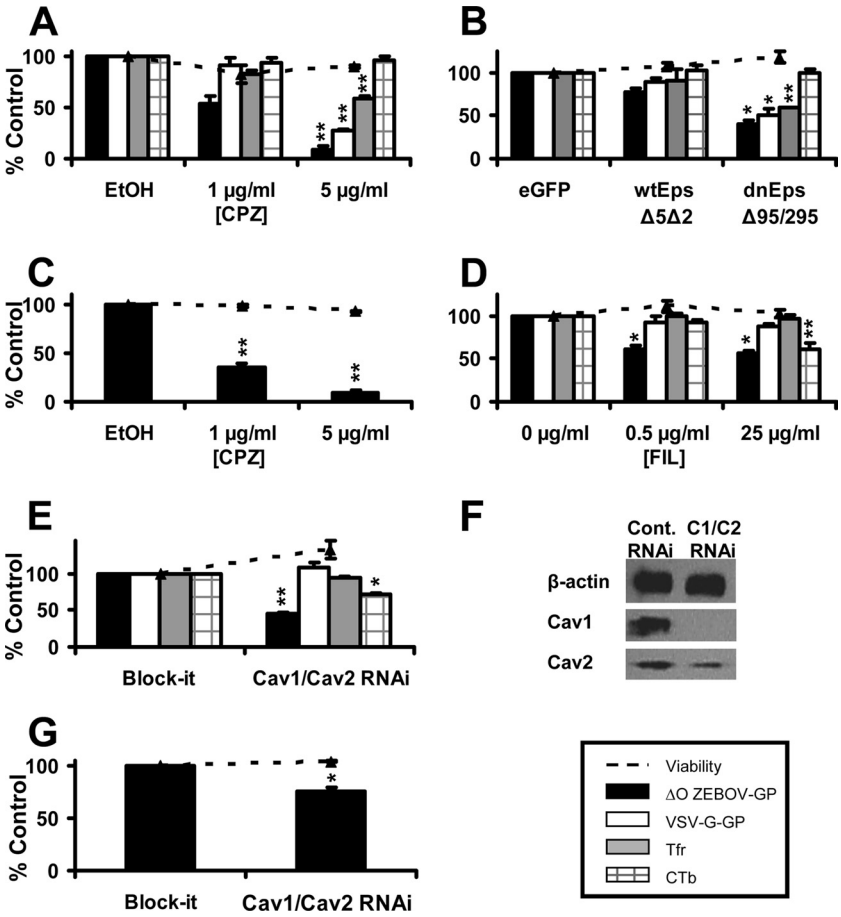

FIG. 2. Clathrin- and caveola/lipid raft-mediated endocytic pathways facilitate FIV-ZEBOV transduction of Axl-dependent cells. (A) Ability of CPZ to inhibit FIV-ZEBOVΔO transduction of SNB19 cells. Cells were pretreated with the indicated amounts of CPZ for 1 h. Treated SNB19 cells were incubated with FIV-ZEBOVΔO (MOI, 0.005), FIV-VSV-G (MOI, 0.005), Cy5-Tfr (20 μg/ml), or Cy5-CTb (10 μg/ml) in the continued presence of CPZ. Tfr- or CTb-treated SNB19 cells were washed after 1 h and analyzed by flow cytometry for uptake of Tfr or CTb. The medium on cells transduced with FIV-ZEBOVΔO or FIV-VSV-G was refreshed after 6 h with medium not containing CPZ, and transduced cells were fixed and stained for β-Gal activity 48 h following transduction. (B) Ability of DNEps15 to inhibit FIV-ZEBOVΔO transduction. SNB19 cells were transfected with plasmid DNA expressing eGFP, wild-type Eps15-GFP (wtEps15), or dominant negative Eps-GFP (DNEps15). The transfection efficiency of SNB19 cells was evaluated at 24 h by analyzing GFP expression in the cells by flow cytometry and was found to be between 50 and 60%. Transfected cells were transduced with FIV-ZEBOVΔO (MOI, 0.005) or FIV-VSV-G (MOI, 0.005) at 24 h following transfection. After an additional 48 h, cells were fixed and stained for β-Gal activity. Alternatively, transfected cells were incubated for 1 h with Cy5-labeled Tfr or CTb and washed and cells were analyzed by flow cytometry for uptake of Tfr and CTb. (C) Ability of CPZ to inhibit FIV-ZEBOV transduction in Hffs. Studies were performed as described for panel A. (D) Ability of FIL to inhibit FIV-ZEBOVΔO transduction into SNB19 cells. Cells were pretreated with the indicated amounts of FIL for 1 h in serum-free medium. The FIL was removed, and cells were incubated with FIV-ZEBOVΔO (MOI, 0.005), FIV-VSV-G (MOI, 0.005), or Cy5-labeled Tfr or CTb in serum-free medium. Tfr- or CTb-treated SNB19 cells were washed after 1 h and analyzed by flow cytometry for uptake of Tfr or CTb. The medium on cells transduced with FIV-ZEBOVΔO or FIV-VSV-G was refreshed after 6 h with medium containing serum without FIL, and transduced cells were fixed and stained for β-Gal activity 48 h following transduction. (E) Knockdown of Cav1/2 inhibits FIV-ZEBOVΔO transduction in SNB19 cells. Cells were transfected with 200 pmol of a nonspecific siRNA control (Block-It) or 200 pmol of a mixture of human Cav1 and Cav 2 siRNAs. At 48 h after transfection, cells were incubated with FIV-ZEBOVΔO, FIV-VSV-G pseudovirions (MOI, 0.005), or Cy5-conjugated Tfr or CTb. After 1 h, the SNB19 cells were analyzed by flow cytometry for uptake of Tfr and CTb. At 48 h following transduction, transduced SNB19 cells were fixed and stained for β-Gal activity. (F) Knockdown of Cav1/2 in SNB19 cells by RNAi. At 48 h after transfection, a portion of the cells were lysed and proteins were separated using SDS-PAGE. Cav1 and Cav2 were detected on the nitrocellulose membrane with primary antibodies (1:1,000 and 1:250, respectively) incubated overnight at 4°C followed by incubation with horseradish peroxidase-conjugated secondary antiserum (1:20,000) for 1 h at room temperature. The blot was visualized by chemiluminescence. Actin was detected by incubation with horseradish peroxidase-conjugated anti-actin antibody (1:10,000). (G) Knockdown of Cav1/2 inhibits FIV-ZEBOVΔO transduction in Hffs. Studies were performed as described for panel E. Cell viability in the presence of the various treatments is shown as a dotted line in panels A to G. Data represent the averages and standard errors of three experiments performed in triplicate. *, $P < 0.05$; **, $P < 0.001$. EtOH, ethanol.

GP-mediated uptake has been previously proposed (4, 22) but also refuted (66). To directly test the role of caveolae, a combination of RNAi specific for human caveolin 1 (Cav1) and caveolin 2 (Cav2) or an irrelevant RNAi control (Block-It) was transfected into SNB19 cells and Hffs. Forty-eight hours after transfection, the efficacy of the RNAi-specific Cav1/2 protein knockdown was determined in a portion of the SNB19 cells (Fig. 2F) and Hff cells (data not shown), and the remaining

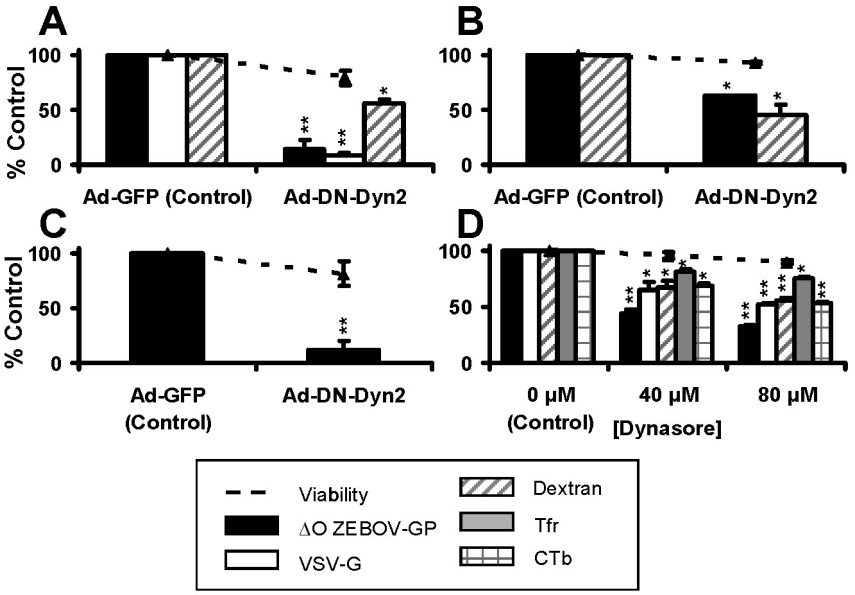

FIG. 3. Dynamin is necessary for efficient ZEBOV-GP pseudovirion entry into Axl-dependent cells. (A to C) Ability of DN dynamin to inhibit FIV-ZEBOVΔO transduction. SNB19 cells (A), Hffs (B), and HuVECs (C) were transduced with adenoviral vectors bearing GFP (Ad-GFP) or a dominant negative form of dynamin 2 (Ad-DN-dyn2) at an MOI of 30 for SNB19 cells and an MOI of 90 for Hffs and HuVECs, ensuring greater than 90% adenovirus transduction. Eighteen hours following adenoviral transduction, SNB19 (A) and Hff (B) cells were incubated with FITC-labeled dextran (0.5-mg/ml final concentration) for 1 h or transduced with FIV pseudovirions (MOI, 0.005; all cell populations) for 48 h. SNB19 and Hff cells were analyzed by flow cytometry for uptake of dextran after 1 h. Transduced cells were fixed and stained for β-Gal activity after 48 h. (D) Ability of Dynasore to inhibit FIV-ZEBOVΔO transduction. SNB19 cells were treated for 1 h with the indicated amounts of Dynasore. Treated cells were incubated with FITC-conjugated dextran or Cy5-conjugated Tfr or CTb for 1 h and analyzed by flow cytometry or incubated with FIV pseudovirions (MOI, 0.005) for an additional 6 h in the presence of the drug. The medium on cells transduced with FIV-ZEBOVΔO or FIV-VSV-G was refreshed after 6 h with medium not containing drug, and transduced cells were fixed and stained for β-Gal activity 48 h following transduction. Cell viability in the presence of the treatments is shown as a dashed line in all panels. Data represent the averages and standard errors of three experiments performed in triplicate. *, $P < 0.05$; **, $P < 0.001$.

cells were transduced with FIV-ZEBOVΔO or FIV-VSV-G. The decrease in Cav1/2 had no effect on VSV-G-dependent transduction but reduced FIV-ZEBOVΔO transduction in SNB19 cells by ~50% (Fig. 2E). These results were confirmed in Hffs by using FIV-ZEBOVΔO (Fig. 2G). Cav1/2 knockdown also decreased CTb uptake but had no effect on Tfr uptake in SNB19 cells (Fig. 2E). Taken together, these findings implicate the use of both clathrin and caveolin pathways by ZEBOV-GP for entry into the Axl-dependent cells.

Dynamin is necessary for efficient ZEBOV-GP pseudovirion entry into Axl-dependent cells. Because both clathrin and lipid raft/caveolin endocytic vesicles require the GTPase dynamin to pinch off endocytic vesicles, we sought to confirm that dynamin was indeed needed for FIV-ZEBOVΔO entry into three cell populations that we have shown to require Axl for transduction (Brindley et al., submitted). SNB19 cells, Hffs, and an additional Axl-dependent primary cell population, human umbilical cord endothelial cells (HuVECs), were transduced with adenovirus (Ad) particles that express GFP or a dominant negative form of dynamin 2 (DNdyn2 [K44A]), since this dynamin isoform is ubiquitously expressed in cells (65). At 24 h following Ad transduction, cells were transduced with FIV-ZEBOVΔO. In our SNB19 cell studies, transduction with FIV-VSV-G served as the positive control since VSV-G-dependent entry into numerous cell types has been shown to be dynamin dependent (3, 5, 35). ZEBOVΔO-GP-mediated entry in SNB19 cells was inhibited by expression of DNdyn2 with a loss of ~85% of transduction (Fig. 3A). Similar results were obtained in HuVECs (Fig. 3C). Interestingly, the effect of DNdyn2 on FIV-ZEBOVΔO entry into Hffs was not as pronounced, causing about 40% inhibition (Fig. 3B). While the effect of DNdyn2 on ZEBOV transduction into Hffs was not as pronounced, the trend was the same as that in SNB19 cells and HuVECs, implicating dynamin-dependent endocytosis mechanisms in ZEBOV transduction. The pan-dynamin inhibitor Dynasore confirmed the importance of dynamin for ZEBOVΔO-GP-dependent transduction in SNB19 cells. This inhibitor significantly reduced ZEBOVΔO-GP- and VSV-G-mediated entry as well as that of Tfr and CTb (Fig. 3D); however, uptake inhibition of pseudovirion transduction by Dynasore was not as pronounced as that which we observed with DNdyn2.

The effect of dynamin inhibitors on Tfr and CTb entry was more modest than the effect on ZEBOV transduction, suggesting that the virus was entering the cells through dynamin-dependent pathways in addition to clathrin- and caveola/lipid raft-mediated endocytosis. Dynamin 2 has been reported not only to be involved in clathrin- and caveola/lipid raft-mediated endocytosis but to be necessary for some forms of coat-independent fluid-phase endocytosis (11). To investigate the role of dynamin dependence in these endocytic pathways, we analyzed uptake of large-molecular-mass, FITC-labeled dextran (70

kDa) in our untreated cells or cells transduced with either a GFP-expressing or a DNdyn2-expressing Ad vector. Dextran has been used extensively to study bulk fluid-phase uptake/macropinocytosis (11, 21, 23, 29, 50). We observed that uptake of dextran in SNB19 cells was decreased by ~40% in the presence of DNdyn (Fig. 3A). Dynasore also inhibited dextran uptake, suggesting that a portion of macropinocytosis (or bulk fluid-phase uptake) in SNB19 cells was indeed dynamin dependent (Fig. 3D). Similar findings were observed in Hffs (Fig. 3B), indicating that dynamin-dependent macropinocytosis was active in the Axl-dependent cells tested.

Inhibitors of macropinocytosis decrease ZEBOV-GP pseudovirion transduction and ZEBOV infection. To assess the impact of macropinocytosis on ZEBOV entry, we first verified that the macropinocytosis-inhibiting drugs reduced dextran uptake in Axl-dependent cells but not uptake of either Tfr or CTb. Three drugs that had previously been used to inhibit macropinocytosis were studied. The amiloride analog EIPA inhibits the Na^+/H^+ exchanger that blocks the formation of macropinosomes during macropinocytosis (50). Blebbistatin (BLB) has been shown to inhibit the formation of myosin II-dependent processes and has been used extensively as an inhibitor of macropinocytosis pathways (38, 44, 50, 64). Cytochalasin B (CYTO-B) inhibits microfilament formation as well as actin polymerization (54). As active actin polymerization is required for macropinocytosis (50), CYTO-B therefore blocks macropinocytosis. Each drug modestly but significantly reduced dextran uptake in SNB19 cells but did not decrease uptake of either Tfr or CTb, demonstrating the specificity of these inhibitors for macropinocytosis in these cells (Fig. 4A).

We next evaluated if these drugs inhibited ZEBOV-GP-mediated transduction. Because VSV-G-mediated entry is thought to be primarily or exclusively due to clathrin-mediated endocytosis, FIV-VSV-G virions served as a negative control in these studies. All three macropinocytosis inhibitors significantly decreased FIV-ZEBOVΔO transduction of SNB19 cells but had no statistically significant effect on FIV-VSV-G transduction relative to the cytotoxicity exhibited by each drug (Fig. 4B to D).

To be sure that the macropinocytosis inhibitors were blocking filovirus entry events, the ability of these drugs to inhibit entry of ZEBOVΔO VLPs into SNB19 cells was assessed. VLPs composed of ZEBOV-VP40 and -GP have the same size and morphology as do infectious filoviruses (19). Our VLPs nonspecifically contained luciferase that was expressed in the producer cell line and incorporated into the VLPs. Fusion of VLPs with endocytic membranes released luciferase, allowing detection of this reporter protein following membrane fusion events (58). Two out of three of the macropinocytosis inhibitors significantly decreased luciferase activity following addition of VLPs to SNB19 cells (Fig. 4E), indicating that the macropinocytosis inhibitors reduce ZEBOV-GP-mediated cell entry.

The two most effective macropinocytosis-inhibiting drugs were then assessed for their ability to inhibit ZEBOV infection of SNB19 cells (Fig. 4F and G). Virus infectivity was assessed by detection of GFP-expressing cells at day 1 of infection. In particular, EIPA profoundly inhibited ZEBOV infection, demonstrating the importance of this pathway for productive filovirus infection of SNB19 cells. Macropinocytosis inhibitors were also observed to block FIV-ZEBOVΔO transduction of Hffs and HeLa cells (data not shown), which had previously been shown to be an Axl-dependent cell line (63). The decrease in filoviral GP-dependent entry by the three macropinocytosis inhibitors was also confirmed using VSV-based pseudovirions bearing full-length forms of either ZEBOV-GP (VSVΔG-ZEBOV-FL) or Lake Victoria MARV-GP (VSVΔG-MARV) (Fig. 4H). These findings collectively indicate that filovirus entry can be mediated through macropinocytotic mechanisms in Axl-dependent cells.

Polymerization of host actin stress fibers is greatly increased following ZEBOV-GP pseudovirion internalization. Because evidence suggested that actin polymerization enhanced filoviral GP-dependent entry, we assessed the presence of F-actin in SNB19 cells by phalloidin staining during FIV-ZEBOVΔO transduction. FIV-ZEBOVΔO pseudovirions (MOI, 250) were bound to cells for 1 h at 4°C. Cells were washed to remove unbound virions, and warmed medium was added to the cells to allow for internalization of the bound virions. At various times, the cells were fixed and immunostained for F-actin and FIV capsid and assessed by confocal microscopy (Fig. 5). A 1-h incubation of virus at 4°C with SNB19 cells allowed us to clearly visualize F-actin and FIV-ZEBOVΔO pseudovirions localized at the periphery of the cells. At 15 min, the localization of the FIV-ZEBOVΔO pseudovirions and F-actin remained unchanged. However, by 30 min, FIV-ZEBOVΔO pseudovirions were located both at the cell periphery and within the cell. By this time point, polymerized actin had increased, resulting in enhanced staining intensity. F-actin was also located throughout the cytoplasm. The increased intensity of F-actin staining was also observed at 45 min, when the majority of the FIV-ZEBOVΔO pseudovirions appeared to be internalized. Together, these data provide further evidence that actin polymerization is involved in filoviral GP-mediated entry.

Inhibition of host PLC inhibits ZEBOV-GP pseudovirion entry into Axl-dependent cells. Recent studies have demonstrated that in addition to inhibiting the formation of clathrin-coated vesicles, the drug CPZ has broader inhibitory activities, interfering with the generation of vesicles such as phagosomes and macropinosomes within cells (36). The mechanism of this activity is believed to be due to CPZ inhibition of one or more isoforms of phospholipase C (PLC) (3). PLC is an important regulator of actin dynamics, and inhibition of PLC activation leads to inhibition of macropinocytosis (1). As a previous study has shown that PLC interacts with phosphorylated tyrosines on the cytoplasmic tail of activated Axl, suggesting that PLC signaling may be a downstream event of Axl activation (48), we investigated the role of CPZ in macropinocytosis inhibition as well as the role of PLC in ZEBOV-GP-mediated entry into SNB19 cells. We observed that CPZ modestly but significantly inhibited the uptake of dextran (Fig. 6A), indicating that in addition to inhibiting clathrin-mediated endocytosis, CPZ also inhibits macropinocytosis activity. The ability of a pan-PLC inhibitor, U-73122, to inhibit FIV-ZEBOVΔO transduction into Axl-dependent and -independent cells was also evaluated. This inhibitor diminished FIV-ZEBOVΔO entry into SNB19 cells (Fig. 6B) and Hffs (data not shown). However, the same concentrations of U-73122 did not inhibit ZEBOV transduction of the Axl-independent cell lines Vero (Fig. 6C) and

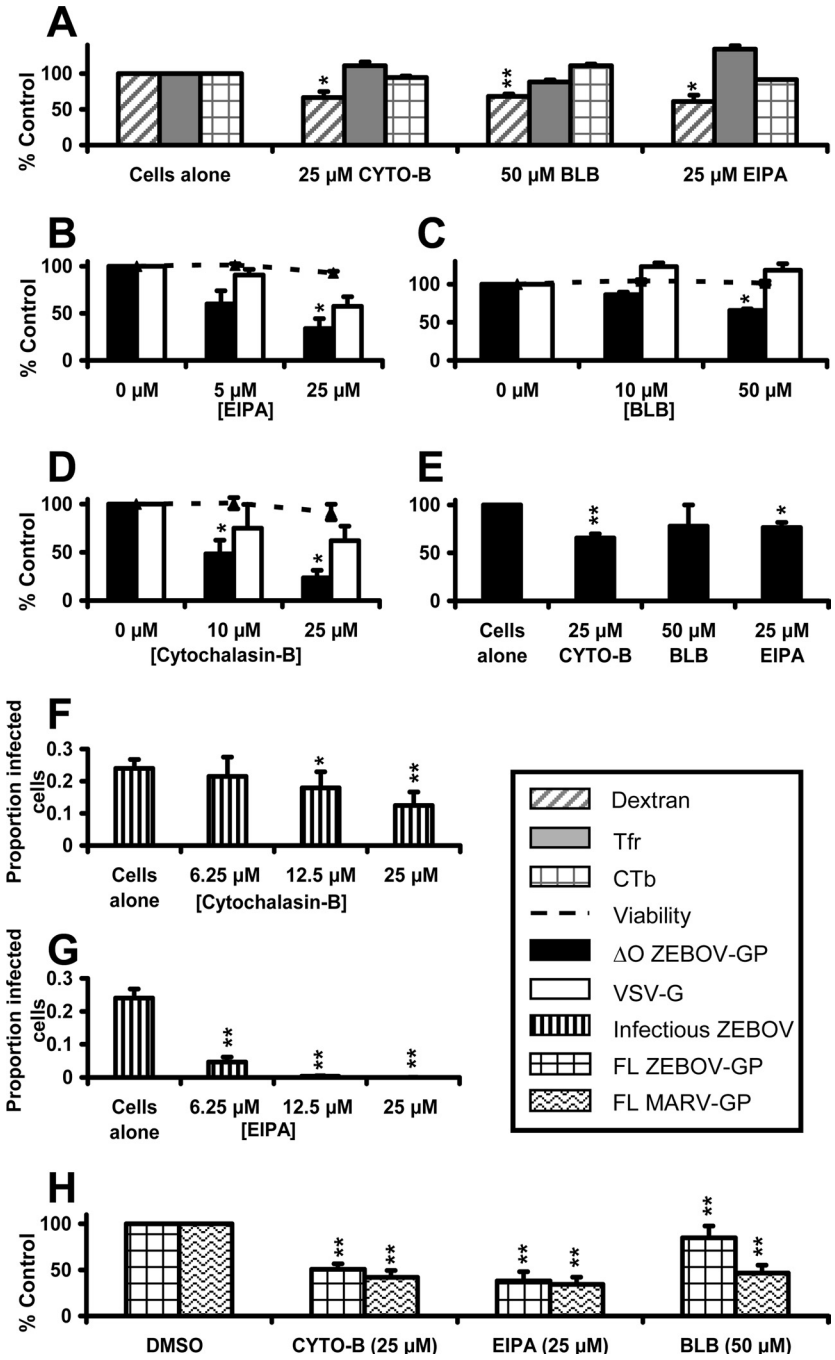

FIG. 4. Inhibitors of macropinocytosis decrease ZEBOV infection in Axl-dependent cells. (A) Ability of macropinocytosis inhibitors to inhibit dextran but not Tfr and CTb uptake. SNB19 cells were treated for 1 h with the indicated amounts of macropinocytosis inhibitors. After 1 h, Cy5-Tfr, Cy5-CTb, or FITC-dextran was added to the cells in the presence of drug for an additional 1 h. The cells were then analyzed by flow cytometry for uptake of the labeled conjugates. (B to D) Ability of macropinocytosis inhibitors to inhibit FIV-ZEBOV transduction. SNB19 cells were incubated for 1 h with the indicated concentrations of macropinocytosis inhibitors. After 1 h, the cells were transduced with FIV pseudovirions (MOI, 0.005) in the presence of the drug for an additional 6 h. Medium was refreshed without drug, and cells were incubated for an additional 48 h. Cells were fixed and stained for β-Gal activity. (E) Ability of macropinocytosis inhibitors to inhibit ZEBOV virus-like particle (VLP) entry into SNB19 cells. SNB19 cells were treated for 1 h with the indicated amounts of macropinocytosis inhibitors. After 1 h, ZEBOV VLPs were added to cells in the presence of drug for an additional 6 h. Unbound VLPs were removed, and cells were lysed and analyzed for luciferase activity. (F and G) Ability of macropinocytosis inhibitors to decrease ZEBOV infection. SNB19 cells were incubated with the indicated concentrations of drug for 1 h. Infectious ZEBOV (MOI, 0.25) was added in the presence of the drug for an additional 17 h. At 17 h following ZEBOV infection, the medium was changed on the cells, and 6 h after that, cells were fixed and assessed by microscopy for GFP positivity relative to the number of cells present for each condition. (H) Indicated amounts of macropinocytosis inhibitors were incubated with SNB19 cells for 1 h. After 1 h, SNB19 cells were transduced with VSVΔG full-length ZEBOV or VSVΔG-MARV-GP (MOI, 0.05). Following 6 h of incubation with virus in medium containing drug, the medium was removed and replaced with medium without drug. VSV-transduced cells were assessed for GFP expression by flow cytometry at 23 h following transduction. Data represent the averages and standard errors of three experiments performed in triplicate. *, $P < 0.05$; **, $P < 0.001$.

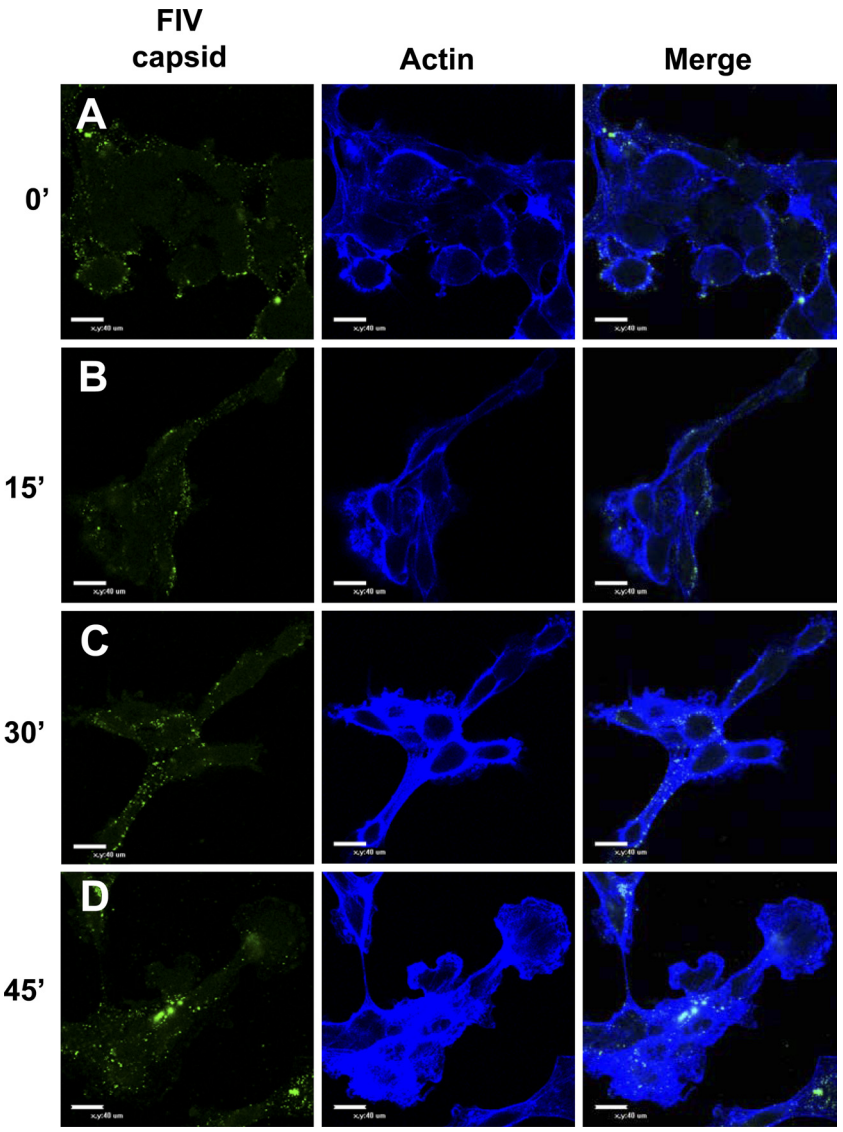

FIG. 5. Actin polymerization increases during FIV-ZEBOVΔO pseudovirion transduction of Axl-dependent SNB19 cells. (A to D) Confocal microscopy of FIV capsid (green) and F-actin (blue) during FIV-ZEBOVΔO pseudovirion transduction (MOI, 250) for 1 h at 4°C (A) or 1 h at 4°C followed by removal of unbound virions and incubation of cells with prewarmed medium at 37°C (B to D) for 15 min (B), 30 min (C), or 45 min (D). Cells were fixed with 2% paraformaldehyde, permeabilized with 0.2% Triton X-100, and immunostained with mouse anti-FIV capsid antibody and Alexa 488-conjugated antiserum. F-actin was detected by staining with Alexa Fluor 647-conjugated phalloidin. Findings shown in panels are representative experiments performed three independent times.

SN12C (data not shown). We have found that Axl expression has no effect on ZEBOV infection of either Vero or SN12C cells (Brindley et al., submitted). Thus, a role for PLC in ZEBOV infection was observed only in cells that required Axl for optimal filovirus entry.

The PLC inhibitor had no effect on FIV-VSV-G entry in any of the cells (Fig. 6B and C). The importance of PLC activity for ZEBOV-GP-mediated entry was confirmed in SNB19 cells by using two additional PLC inhibitors, ET-18-OCH_3 and D609. Both drugs significantly inhibited FIV-ZEBOVΔO transduction in SNB19 cells at the 50% inhibitory concentration (IC_{50}) of each drug (~15 μM) (40) and at a higher concentration, 50 μM (data not shown). Together, these results clearly show a specific involvement of PLC activity for ZEBOV-GP-mediated entry into cells that require Axl for ZEBOV infection but not in cells that do not have this dependence.

Axl signaling is also known to be mediated through phosphoinositide 3-kinase (PI3K) (48). In addition, ZEBOV entry into the Axl-independent VeroE6 cells requires PI3K activity (58). Consequently, in parallel with our PLC studies, we evaluated whether FIV-ZEBOVΔO transduction was decreased in the presence of the PI3K inhibitor LY-294,002. This inhibitor had no effect on ZEBOV-GP-mediated entry into SNB19 cells (Fig. 6D) or Hffs (data not shown) but decreased FIV-ZEBOVΔO transduction into Axl-independent Vero (Fig. 6E) and SN12C (data not shown) cells. VSV-G-dependent entry into all cells tested was unaffected by LY-294,002 (Fig. 6D and E). In total, our findings indicate that signaling through PLC

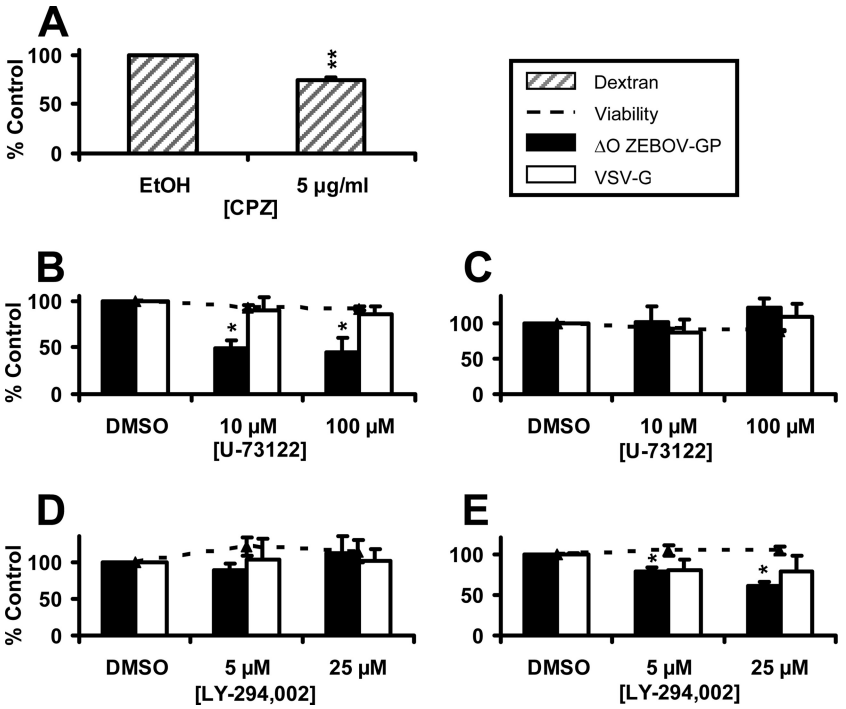

FIG. 6. Phospholipase C activation enhances ZEBOV-GP-mediated entry into Axl-dependent cells but not Axl-independent cells. (A) Ability of CPZ to inhibit dextran uptake. SNB19 cells were incubated with the indicated amounts of CPZ for 1 h. After 1 h, FITC-labeled dextran was added in the presence of the drug. Dextran-treated cells were washed after 1 h and analyzed by flow cytometry for uptake of dextran. (B to E) Ability of a PLC inhibitor, but not a PI3K inhibitor, to inhibit FIV-ZEBOV transduction of Axl-dependent cells. SNB19 cells (B and D) or Vero cells (C and E) were treated for 1 h with the indicated amounts of kinase inhibitor. Cells were then incubated with FIV pseudovirions (MOI, 0.005) in the continued presence of drug. The medium was changed after 6 h, and transduced cells were fixed and stained for β-Gal activity 48 h following transduction. Data represent the averages and standard errors of three experiments performed in triplicate. *, $P < 0.05$; **, $P < 0.001$.

but not PI3K is necessary for optimal ZEBOV-GP-mediated entry into Axl-dependent cells. In contrast, as others have shown (58), PI3K activity is needed for ZEBOV-GP-mediated entry into Vero cells.

Axl facilitates macropinocytosis of ZEBOV-GP pseudovirions. To determine if one or more of the ZEBOV-GP-mediated entry pathways was altered by the loss of Axl expression, Axl was knocked down by Axl RNAi in SNB19 cells and the impact of that knockdown on macropinocytosis as well as clathrin- and caveola/lipid raft-mediated endocytic events was evaluated. Reduction of Axl expression in SNB19 cells decreased uptake of dextran but not Tfr or CTb, suggesting that Axl specifically modulates macropinocytosis within these cells (Fig. 7A). To determine if loss of Axl was affecting macropinocytosis-dependent FIV-ZEBOVΔO transduction, we evaluated FIV-ZEBOVΔO transduction in the presence of both macropinocytosis inhibitors and Axl RNAi, anticipating that loss of Axl expression would lead to an abrogation of macropinocytosis inhibitor effects. As shown in Fig. 1, we observed that Axl RNAi treatment inhibited ~80% of ZEBOV-GP-dependent transduction. The transduction level in both the Axl RNAi-treated cells and the irrelevant control RNAi-treated cells was set to 100%, providing a no-drug control for these studies. We then tested the impact of the addition of CYTO-B, BLB, and EIPA on FIV-ZEBOVΔO transduction of the RNAi-treated cell populations. While FIV-ZEBOVΔO transduction of the irrelevant RNAi-treated cells was inhibited by each of the macropinocytosis inhibitors as we had observed earlier, loss of Axl expression led to a reduced effect of each of the macropinocytosis inhibitors (Fig. 7B). In fact, CYTO-B and BLB had no effect on Axl RNAi-treated cells, whereas EIPA remained somewhat inhibitory even in the presence of Axl RNAi (Fig. 7B). It is possible that EIPA is inhibiting additional endocytic pathways independently of Axl (27). When adjusted for cytotoxicity, the combination of Axl RNAi and macropinocytosis inhibitors had no effect on FIV-VSV-G entry (Fig. 7C). This finding was anticipated since neither Axl RNAi nor the macropinocytosis inhibitors alone affected VSV-G-dependent transduction in SNB19 cells. Together, these data provide strong evidence that Axl stimulates macropinocytosis in some cell populations. This enhancement leads to greater levels of ZEBOV transduction through one or more macropinocytotic pathways, thus assigning a specific role for Axl in filoviral entry for the first time.

DISCUSSION

Knockdown of Axl in SNB19 cells abrogated approximately 80% of filovirus infectivity, demonstrating for the first time the importance of endogenous expression of this protein for filovirus infection. With the appreciation that Axl expression is critical for filovirus infection in some cells, this study sought to identify an uptake pathway(s) used by ZEBOV for entry into cells that require Axl for optimal infection and to determine if

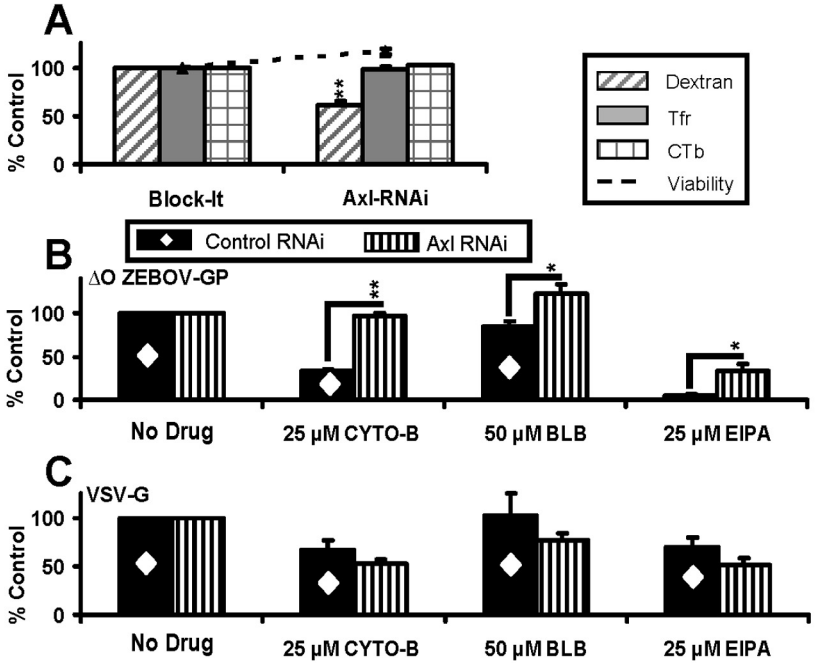

FIG. 7. Axl facilitates macropinocytosis into SNB19 cells. (A) Ability of Axl RNAi to inhibit dextran but not Tfr and CTb uptake. SNB19 cells were transfected with 200 pmol of a nonspecific siRNA control (Block-It) or 200 pmol of a human Axl-specific siRNA. At 48 h following RNAi transfection, cells were incubated for 1 h with Cy5-Tfr, Cy5-CTb, or FITC-dextran. After 1 h, cells were analyzed by flow cytometry for uptake of labeled conjugates. (B) Macropinocytosis inhibitors do not inhibit FIV-ZEBOV transduction when Axl is knocked down by RNAi in SNB19 cells. SNB19 cells were transfected with Axl siRNA or control siRNA (Block-It; Invitrogen). At 48 h posttransfection, cells were treated for 1 h with the indicated amounts of macropinocytosis inhibitors. Treated cells were transduced with FIV-ZEBOVΔO (MOI, 0.005) for an additional 6 h in the presence of drugs. The medium was refreshed after 6 h with medium not containing drug, and transduced cells were fixed and stained for β-Gal activity at 48 h following transduction. ZEBOV-GP-mediated transduction of cells transfected with an irrelevant RNAi is about 4-fold higher than that observed in the presence of Axl RNAi. Each of these transduction values was set to 100% (No Drug), and we assessed the effect of macropinocytosis inhibitors on ZEBOV-GP pseudovirion transduction in the presence or absence of Axl expression relative to these controls. (C) Macropinocytosis inhibitors have no effect on FIV-VSV-G transduction in the presence or absence of Axl in SNB19 cells. Studies were performed as described for panel B, but FIV-VSV-G (MOI, 0.005) was transduced. Data represent the averages and standard errors of three experiments performed in triplicate. *, $P < 0.05$; **, $P < 0.001$.

Axl impacted those uptake pathways used. Here, we demonstrated in cells that require Axl for optimal filovirus GP-dependent entry that infection can occur through multiple mechanisms, including clathrin- and caveola/lipid raft-mediated endocytosis and macropinocytosis (Fig. 8). Reduction of Axl expression decreased the ability of macropinocytosis inhibitors to block ZEBOV transduction, implicating Axl in stimulating macropinocytosis. As Axl signaling has been predicted to activate PLC, which in turn enhances macropinocytosis (1), we evaluated if ZEBOV entry was inhibited by PLC inhibitors. Indeed, we observed a reduction in ZEBOV entry in the presence of three different PLC inhibitors, demonstrating a requirement for PLC signaling during ZEBOV transduction of Axl-requiring cells. A similar dependence of PLC signaling was not observed for ZEBOV transduction into Vero cells that do not require Axl for filoviral infection. Thus, we propose that Axl expression enhances ZEBOV entry through PLC signaling, leading to enhanced macropinocytosis. These studies identify a mechanistic role for Axl in filovirus entry for the first time.

Recently, others have also demonstrated that macropinocytosis is involved in filoviral entry into several cell populations that do not require Axl for filovirus infection, including Vero, VeroE6, and HEK 293T cells (51, 57). Signals that stimulate bulk fluid-phase uptake in these cells have not been defined but must differ from the Axl-dependent signals that we identify in these studies. Interestingly, in contrast to previously published data, Saeed et al. found that infectious ZEBOV entry into both HEK 293T and VeroE6 cells was independent of clathrin- and caveola-mediated endocytosis but involved a "macropinocytosis-like" endocytic event (57). It has been previously suggested that filoviruses may use different receptors for productive internalization into different cell populations (33). If this proves to be the situation, routes of entry might be expected to differ in these various cell populations depending on the receptor utilized by the virus.

Here, we clearly demonstrate a role for Axl in stimulating macropinocytosis in some cells. Decreased Axl expression by RNAi led to reduced dextran uptake as well as ZEBOV entry but did not alter uptake of Tfr, CTb, or VSV-G-expressing pseudovirions. Peptides from the Axl cytoplasmic tail containing phosphorylated Y821 or Y866 are postulated to serve as docking sites for PLCγ (48), and activation of PLC leads to enhanced bulk fluid uptake in some cells via an enhancement of actin polymerization (1). Our microscopy data strongly suggest that actin polymerization is triggered as

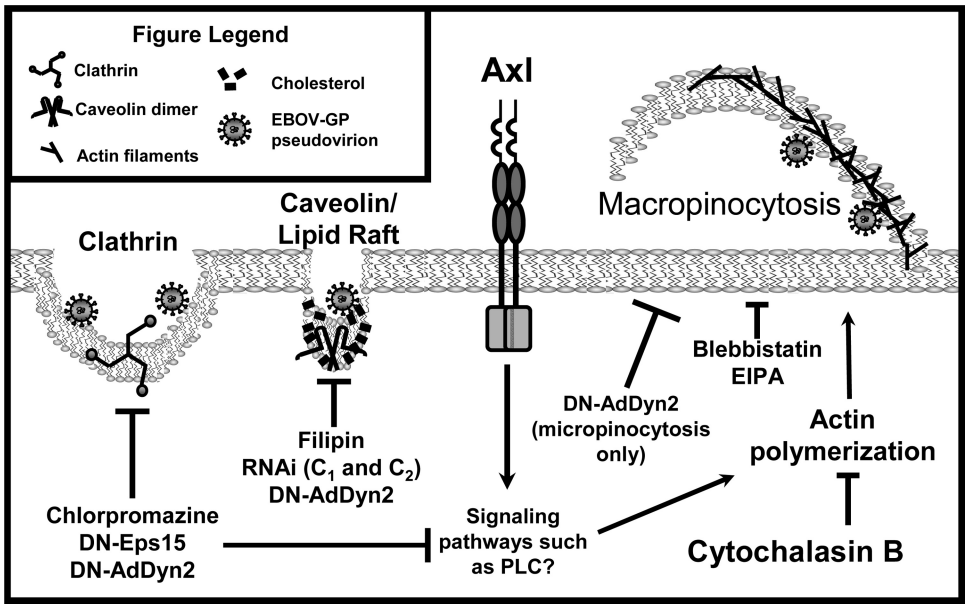

FIG. 8. Model for ZEBOV-GP-mediated entry into Axl-dependent cells. ZEBOV-GP-mediated entry into Axl-dependent cells occurs through multiple mechanisms as evidenced by the use of biochemical inhibitors, dominant negative forms of endocytic proteins, and RNAi. These routes of entry include the use of clathrin-coated pits, caveolae, lipid rafts, and dynamin-dependent and -independent macropinocytosis. Inhibition of ZEBOV-GP-mediated entry by each of the endocytic inhibitors was incomplete, indicating that multiple entry mechanisms are used by ZEBOV-GP. Axl signaling through PLC but not PI3K promotes efficient ZEBOV-GP-mediated entry in Axl-dependent cells, indicating that Axl is capable of serving as a signaling platform through which ZEBOV-GP indirectly mediates entry via macropinocytosis.

ZEBOV pseudovirions are internalized into SNB19 cells. Therefore, it is tempting to speculate that direct Axl/PLC interactions lead to signaling events that result in increased actin polymerization and enhanced macropinocytosis. Enhancement of macropinocytosis by Tyro3/Axl/Mer (TAM) receptor signaling in our studies is consistent with increased phagocytosis and clearance of apoptotic cells in professional phagocytic cells following TAM signaling (7). However, to date a role for any TAM family member in signal-induced macropinocytosis in a nonprofessional phagocytic cell population has not been shown. This study provides compelling evidence that the presence of Axl stimulates macropinocytosis in cells that have enhanced ZEBOV-GP-mediated entry in the presence of Axl.

Mechanisms leading to Axl signaling during ZEBOV-GP-dependent entry that enhance macropinocytosis remain unknown. Because no direct interaction between any filoviral GP and Axl has been shown, it leaves open the possibility that an indirect interaction may be occurring. The possibility also exists that Axl may be capable of acting in concert with other TAM family molecules or other receptors to elicit ZEBOV entry.

Despite the fact that Vero cells express cell surface Axl, Axl expression has no impact on filovirus infection of this cell line (63). This suggests that pathways connecting Axl to macropinocytosis may be disrupted in this cell line. The requirement of PI3K/Akt signaling for filovirus infection in this line that we and others (58) have shown may abrogate the need for an intact Axl signaling pathway.

Many of the inhibitors that were tested only partially inhibited ZEBOV entry, reducing virus uptake by 25 to 75%. Incomplete abrogation of ZEBOV entry with any single inhibitor provides evidence that multiple, independent mechanisms of uptake can be used by ZEBOV-GP for entry into these cells. As previous studies have demonstrated that inhibition of one uptake pathway can enhance uptake activity through other pathways (60), it is likely that this compensation mechanism is occurring and may explain the moderate levels of inhibition observed in our studies.

Interestingly, one of the macropinocytosis-inhibiting drugs tested (EIPA) retained a partial ability to decrease ZEBOV entry in the Axl-dependent SNB19 cells during Axl RNAi knockdown (Fig. 7B). This suggests that EIPA may also be inhibiting one or more uptake pathways that are independent of Axl regulation. Such pathways could include Axl-independent macropinocytosis pathways as well as other endocytotic pathways, although neither uptake of Tfr nor that of CTb was decreased by EIPA treatment in this study (Fig. 4A). Indeed, earlier studies have shown that inhibition by EIPA or another amiloride analog can block albumin uptake through "receptor-mediated events" which may not include macropinocytotic events (26, 27).

Not only does Axl enhance macropinocytosis-mediated ZEBOV entry, ectopic expression of RhoB or RhoC is also capable of enhancing macropinocytosis, leading to increased FIV-ZEBOVΔO transduction (56). In the case of the Rho proteins, enhancement is not specific for ZEBOV since VSV-G pseudovirion transduction and VSV infection are also dramatically increased. In contrast, we observed specific enhancement of ZEBOV entry by Axl in SNB19 cells. Thus, Axl-dependent enhancement and Rho-dependent enhancement of macropinocytosis may result from activation of partially or completely different signaling pathways. Alternatively, Rho-dependent macropinocytosis enhancement may occur downstream from Axl-dependent events and, when Rho is overexpressed,

macropinocytosis activation becomes independent of cell surface interactions.

Clathrin-coated vesicles have an average diameter of ~120 nm, whereas caveola vesicles have a diameter of ~60 to 80 nm (14). Cargoes taken up by these endocytic vesicles are generally thought to be limited, in part, by the size of the endocytic vesicle formed, although a recent study suggests that incomplete coating of clathrin pits may allow larger cargoes to enter these vesicles (16). The length of filoviral particles (800 to 1,400 nm) has the potential to hinder ZEBOV from utilizing these uptake mechanisms. However, several reports indicate that one or both of these pathways are important for ZEBOV infection of some cells (6, 59). Our pseudovirion studies support the ability of the filoviral glycoproteins to mediate lentiviral particle entry via these endocytic pathways as well as through macropinocytosis. As ZEBOVΔO-GP has been used as a viral glycoprotein to pseudotype lentiviral gene therapy vectors into cells (47, 68), these studies provide insights into multiple uptake pathways that such vectors may use.

In contrast to the potential size restriction of clathrin-dependent and caveola/lipid raft-mediated endocytosis, size constraints of cargo are not an issue for bulk fluid-phase uptake pathways such as macropinocytosis where particles larger than 1 μm in size can be internalized into cells (2). Vesicles generated by these uptake pathways also have the ability to become acidified and interact with endocytic vesicles (32) and therefore could fulfill the requirement of a low-pH step that is essential for filovirus entry. To date, several other viruses have been shown to utilize macropinocytosis mechanisms to enter host cells, including vaccinia virus and human immunodeficiency virus type 1 (50). The evidence presented here confirms recent findings that macropinocytosis is a route for productive filoviral entry (51, 57) and definitively designates a role for Axl in this process.

ACKNOWLEDGMENTS

We thank Melinda Brindley and John A. Chiorini for critically reviewing the manuscript.

These studies have been supported by NIH grants AI73306 and AI082409 (W.M.) and AI057156 (R.A.D.).

REFERENCES

1. **Amyere, M., B. Payrastre, U. Krause, P. Van Der Smissen, A. Veithen, and P. J. Courtoy.** 2000. Constitutive macropinocytosis in oncogene-transformed fibroblasts depends on sequential permanent activation of phosphoinositide 3-kinase and phospholipase C. Mol. Biol. Cell **11:**3453–3467.
2. **Ascenzi, P., A. Bocedi, J. Heptonstall, M. R. Capobianchi, A. Di Caro, E. Mastrangelo, M. Bolognesi, and G. Ippolito.** 2008. Ebolavirus and Marburgvirus: insight the Filoviridae family. Mol. Aspects Med. **29:**151–185.
3. **Basta-Kaim, A., B. Budziszewska, L. Jaworska-Feil, M. Tetich, M. Leskiewicz, M. Kubera, and W. Lason.** 2002. Chlorpromazine inhibits the glucocorticoid receptor-mediated gene transcription in a calcium-dependent manner. Neuropharmacology **43:**1035–1043.
4. **Bavari, S., C. M. Bosio, E. Wiegand, G. Ruthel, A. B. Will, T. W. Geisbert, M. Hevey, C. Schmaljohn, A. Schmaljohn, and M. J. Aman.** 2002. Lipid raft microdomains: a gateway for compartmentalized trafficking of Ebola and Marburg viruses. J. Exp. Med. **195:**593–602.
5. **Benmerah, A., M. Bayrou, N. Cerf-Bensussan, and A. Dautry-Varsat.** 1999. Inhibition of clathrin-coated pit assembly by an Eps15 mutant. J. Cell Sci. **112:**1303–1311.
6. **Bhattacharyya, S., K. L. Warfield, G. Ruthel, S. Bavari, M. J. Aman, and T. J. Hope.** 2010. Ebola virus uses clathrin-mediated endocytosis as an entry pathway. Virology **401:**18–28.
7. **Binder, M. D., and T. J. Kilpatrick.** 2009. TAM receptor signalling and demyelination. Neurosignals **17:**277–287.
8. **Bray, M., S. Hatfill, L. Hensley, and J. W. Huggins.** 2001. Haematological, biochemical and coagulation changes in mice, guinea-pigs and monkeys infected with a mouse-adapted variant of Ebola Zaire virus. J. Comp. Pathol. **125:**243–253.
9. **Brindley, M. A., L. Hughes, A. Ruiz, P. B. McCray, Jr., A. Sanchez, D. A. Sanders, and W. Maury.** 2007. Ebola virus glycoprotein 1: identification of residues important for binding and postbinding events. J. Virol. **81:**7702–7709.
10. **Brindley, M. A., and W. Maury.** 2008. Equine infectious anemia virus entry occurs through clathrin-mediated endocytosis. J. Virol. **82:**1628–1637.
11. **Cao, H., J. Chen, M. Awoniyi, J. R. Henley, and M. A. McNiven.** 2007. Dynamin 2 mediates fluid-phase micropinocytosis in epithelial cells. J. Cell Sci. **120:**4167–4177.
12. **Centers for Disease Control and Prevention.** 2009. Imported case of Marburg hemorrhagic fever—Colorado, 2008. MMWR Morb. Mortal. Wkly. Rep. **58:**1377–1381.
13. **Chandran, K., N. J. Sullivan, U. Felbor, S. P. Whelan, and J. M. Cunningham.** 2005. Endosomal proteolysis of the Ebola virus glycoprotein is necessary for infection. Science **308:**1643–1645.
14. **Conner, S. D., and S. L. Schmid.** 2003. Regulated portals of entry into the cell. Nature **422:**37–44.
15. **Connolly, B. M., K. E. Steele, K. J. Davis, T. W. Geisbert, W. M. Kell, N. K. Jaax, and P. B. Jahrling.** 1999. Pathogenesis of experimental Ebola virus infection in guinea pigs. J. Infect. Dis. **179**(Suppl. 1)**:**S203–S217.
16. **Cureton, D. K., R. H. Massol, S. Saffarian, T. L. Kirchhausen, and S. P. Whelan.** 2009. Vesicular stomatitis virus enters cells through vesicles incompletely coated with clathrin that depend upon actin for internalization. PLoS Pathog. **5:**e1000394.
17. **Davis, K. J., A. O. Anderson, T. W. Geisbert, K. E. Steele, J. B. Geisbert, P. Vogel, B. M. Connolly, J. W. Huggins, P. B. Jahrling, and N. K. Jaax.** 1997. Pathology of experimental Ebola virus infection in African green monkeys. Involvement of fibroblastic reticular cells. Arch. Pathol. Lab. Med. **121:**805–819.
18. **Doherty, G. J., and H. T. McMahon.** 2009. Mechanisms of endocytosis. Annu. Rev. Biochem. **78:**857–902.
19. **Dolnik, O., L. Kolesnikova, and S. Becker.** 2008. Filoviruses: interactions with the host cell. Cell. Mol. Life Sci. **65:**756–776.
20. **Donaldson, J. G., N. Porat-Shliom, and L. A. Cohen.** 2009. Clathrin-independent endocytosis: a unique platform for cell signaling and PM remodeling. Cell. Signal. **21:**1–6.
21. **Ellerbroek, S. M., K. Wennerberg, W. T. Arthur, J. M. Dunty, D. R. Bowman, K. A. DeMali, C. Der, and K. Burridge.** 2004. SGEF, a RhoG guanine nucleotide exchange factor that stimulates macropinocytosis. Mol. Biol. Cell **15:**3309–3319.
22. **Empig, C. J., and M. A. Goldsmith.** 2002. Association of the caveola vesicular system with cellular entry by filoviruses. J. Virol. **76:**5266–5270.
23. **Falcone, S., E. Cocucci, P. Podini, T. Kirchhausen, E. Clementi, and J. Meldolesi.** 2006. Macropinocytosis: regulated coordination of endocytic and exocytic membrane traffic events. J. Cell Sci. **119:**4758–4769.
24. **Geisbert, T. W., and N. K. Jaax.** 1998. Marburg hemorrhagic fever: report of a case studied by immunohistochemistry and electron microscopy. Ultrastruct. Pathol. **22:**3–17.
25. **Geisbert, T. W., P. B. Jahrling, M. A. Hanes, and P. M. Zack.** 1992. Association of Ebola-related Reston virus particles and antigen with tissue lesions of monkeys imported to the United States. J. Comp. Pathol. **106:**137–152.
26. **Gekle, M., K. Drumm, S. Mildenberger, R. Freudinger, B. Gassner, and S. Silbernagl.** 1999. Inhibition of Na+-H+ exchange impairs receptor-mediated albumin endocytosis in renal proximal tubule-derived epithelial cells from opossum. J. Physiol. **520:**709–721.
27. **Gekle, M., R. Freudinger, and S. Mildenberger.** 2001. Inhibition of Na+-H+ exchanger-3 interferes with apical receptor-mediated endocytosis via vesicle fusion. J. Physiol. **531:**619–629.
28. **Gibb, T. R., M. Bray, T. W. Geisbert, K. E. Steele, W. M. Kell, K. J. Davis, and N. K. Jaax.** 2001. Pathogenesis of experimental Ebola Zaire virus infection in BALB/c mice. J. Comp. Pathol. **125:**233–242.
29. **Gold, S., P. Monaghan, P. Mertens, and T. Jackson.** 2010. A clathrin independent macropinocytosis-like entry mechanism used by bluetongue virus-1 during infection of BHK cells. PLoS One **5:**e11360.
30. **Gonzalez, J. P., X. Pourrut, and E. Leroy.** 2007. Ebolavirus and other filoviruses. Curr. Top. Microbiol. Immunol. **315:**363–387.
31. **Groseth, A., H. Feldmann, and J. E. Strong.** 2007. The ecology of Ebola virus. Trends Microbiol. **15:**408–416.
32. **Hewlett, L. J., A. R. Prescott, and C. Watts.** 1994. The coated pit and macropinocytic pathways serve distinct endosome populations. J. Cell Biol. **124:**689–703.
33. **Hoenen, T., A. Groseth, D. Falzarano, and H. Feldmann.** 2006. Ebola virus: unravelling pathogenesis to combat a deadly disease. Trends Mol. Med. **12:**206–215.
34. **Hooper, N. M.** 1999. Detergent-insoluble glycosphingolipid/cholesterol-rich membrane domains, lipid rafts and caveolae. Mol. Membr. Biol. **16:**145–156.
35. **Iannolo, G., A. E. Salcini, I. Gaidarov, O. B. Goodman, Jr., J. Baulida, G. Carpenter, P. G. Pelicci, P. P. Di Fiore, and J. H. Keen.** 1997. Mapping of the molecular determinants involved in the interaction between eps15 and AP-2. Cancer Res. **57:**240–245.

36. **Ivanov, A. I.** 2008. Pharmacological inhibition of endocytic pathways: is it specific enough to be useful? Methods Mol. Biol. **440:**15–33.
37. **Jeffers, S. A., D. A. Sanders, and A. Sanchez.** 2002. Covalent modifications of the Ebola virus glycoprotein. J. Virol. **76:**12463–12472.
38. **Jiang, J., A. L. Kolpak, and Z. Z. Bao.** 2010. Myosin IIB isoform plays an essential role in the formation of two distinct types of macropinosomes. Cytoskeleton (Hoboken) **67:**32–42.
39. **Johannsdottir, H. K., R. Mancini, J. Kartenbeck, L. Amato, and A. Helenius.** 2009. Host cell factors and functions involved in vesicular stomatitis virus entry. J. Virol. **83:**440–453.
40. **Journal of Cellular Biochemistry.** 1994. Lipid second messengers. Keystone Symposium. Taos, New Mexico, February 26-March 4, 1994. Abstracts. J. Cell. Biochem. Suppl. **18D:**19–63.
41. **Kao, A. W., B. P. Ceresa, S. R. Santeler, and J. E. Pessin.** 1998. Expression of a dominant interfering dynamin mutant in 3T3L1 adipocytes inhibits GLUT4 endocytosis without affecting insulin signaling. J. Biol. Chem. **273:** 25450–25457.
42. **Kuhn, J. H., S. R. Radoshitzky, A. C. Guth, K. L. Warfield, W. Li, M. J. Vincent, J. S. Towner, S. T. Nichol, S. Bavari, H. Choe, M. J. Aman, and M. Farzan.** 2006. Conserved receptor-binding domains of Lake Victoria marburgvirus and Zaire ebolavirus bind a common receptor. J. Biol. Chem. **281:**15951–15958.
43. **Kuzmin, I. V., M. Niezgoda, R. Franka, B. Agwanda, W. Markotter, R. F. Breiman, W. J. Shieh, S. R. Zaki, and C. E. Rupprecht.** 2010. Marburg virus in fruit bat, Kenya. Emerg. Infect. Dis. **16:**352–354.
44. **Laliberte, J. P., and B. Moss.** 2009. Appraising the apoptotic mimicry model and the role of phospholipids for poxvirus entry. Proc. Natl. Acad. Sci. U. S. A. **106:**17517–17521.
45. **Leroy, E. M., A. Epelboin, V. Mondonge, X. Pourrut, J. P. Gonzalez, J. J. Muyembe-Tamfum, and P. Formenty.** 2009. Human Ebola outbreak resulting from direct exposure to fruit bats in Luebo, Democratic Republic of Congo, 2007. Vector Borne Zoonotic Dis. **9:**723–728.
46. **Leroy, E. M., B. Kumulungui, X. Pourrut, P. Rouquet, A. Hassanin, P. Yaba, A. Delicat, J. T. Paweska, J. P. Gonzalez, and R. Swanepoel.** 2005. Fruit bats as reservoirs of Ebola virus. Nature **438:**575–576.
47. **Limberis, M. P., C. L. Bell, J. Heath, and J. M. Wilson.** 2010. Activation of transgene-specific T cells following lentivirus-mediated gene delivery to mouse lung. Mol. Ther. **18:**143–150.
48. **Linger, R. M., A. K. Keating, H. S. Earp, and D. K. Graham.** 2008. TAM receptor tyrosine kinases: biologic functions, signaling, and potential therapeutic targeting in human cancer. Adv. Cancer Res. **100:**35–83.
49. **Manicassamy, B., J. Wang, H. Jiang, and L. Rong.** 2005. Comprehensive analysis of Ebola virus GP1 in viral entry. J. Virol. **79:**4793–4805.
50. **Mercer, J., and A. Helenius.** 2009. Virus entry by macropinocytosis. Nat. Cell Biol. **11:**510–520.
51. **Nanbo, A., M. Imai, S. Watanabe, T. Noda, K. Takahashi, G. Neumann, P. Halfmann, and Y. Kawaoka.** 2010. Ebolavirus is internalized into host cells via macropinocytosis in a viral glycoprotein-dependent manner. PLoS Pathog. **6**(9)**:**e1001121.
52. **Neumann, G., H. Feldmann, S. Watanabe, I. Lukashevich, and Y. Kawaoka.** 2002. Reverse genetics demonstrates that proteolytic processing of the Ebola virus glycoprotein is not essential for replication in cell culture. J. Virol. **76:**406–410.
53. **Orlandi, P. A., and P. H. Fishman.** 1998. Filipin-dependent inhibition of cholera toxin: evidence for toxin internalization and activation through caveolae-like domains. J. Cell Biol. **141:**905–915.
54. **Peterson, J. R., and T. J. Mitchison.** 2002. Small molecules, big impact: a history of chemical inhibitors and the cytoskeleton. Chem. Biol. **9:**1275–1285.
55. **Pourrut, X., M. Souris, J. S. Towner, P. E. Rollin, S. T. Nichol, J. P. Gonzalez, and E. Leroy.** 2009. Large serological survey showing cocirculation of Ebola and Marburg viruses in Gabonese bat populations, and a high seroprevalence of both viruses in Rousettus aegyptiacus. BMC Infect. Dis. **9:**159.
56. **Quinn, K., M. A. Brindley, M. L. Weller, N. Kaludov, A. Kondratowicz, C. L. Hunt, P. L. Sinn, P. B. McCray, Jr., C. S. Stein, B. L. Davidson, R. Flick, R. Mandell, W. Staplin, W. Maury, and J. A. Chiorini.** 2009. Rho GTPases modulate entry of Ebola virus and vesicular stomatitis virus pseudotyped vectors. J. Virol. **83:**10176–10186.
57. **Saeed, M. F., A. A. Kolokoltsov, T. Albrecht, and R. A. Davey.** 2010. Cellular entry of ebola virus involves uptake by a macropinocytosis-like mechanism and subsequent trafficking through early and late endosomes. PLoS Pathog. **6**(9)**:**e1001110.
58. **Saeed, M. F., A. A. Kolokoltsov, A. N. Freiberg, M. R. Holbrook, and R. A. Davey.** 2008. Phosphoinositide-3 kinase-Akt pathway controls cellular entry of Ebola virus. PLoS Pathog. **4:**e1000141.
59. **Sanchez, A.** 2007. Analysis of filovirus entry into Vero e6 cells, using inhibitors of endocytosis, endosomal acidification, structural integrity, and cathepsin (B and L) activity. J. Infect. Dis. **196**(Suppl. 2)**:**S251–S258.
60. **Schaeffer, E., V. B. Soros, and W. C. Greene.** 2004. Compensatory link between fusion and endocytosis of human immunodeficiency virus type 1 in human CD4 T lymphocytes. J. Virol. **78:**1375–1383.
61. **Schornberg, K., S. Matsuyama, K. Kabsch, S. Delos, A. Bouton, and J. White.** 2006. Role of endosomal cathepsins in entry mediated by the Ebola virus glycoprotein. J. Virol. **80:**4174–4178.
62. **Schornberg, K. L., C. J. Shoemaker, D. Dube, M. Y. Abshire, S. E. Delos, A. H. Bouton, and J. M. White.** 2009. Alpha5beta1-integrin controls Ebolavirus entry by regulating endosomal cathepsins. Proc. Natl. Acad. Sci. U. S. A. **106:**8003–8008.
63. **Shimojima, M., A. Takada, H. Ebihara, G. Neumann, K. Fujioka, T. Irimura, S. Jones, H. Feldmann, and Y. Kawaoka.** 2006. Tyro3 family mediated cell entry of Ebola and Marburg viruses. J. Virol. **80:**10109–10116.
64. **Shu, S., X. Liu, and E. D. Korn.** 2005. Blebbistatin and blebbistatin-inactivated myosin II inhibit myosin II-independent processes in Dictyostelium. Proc. Natl. Acad. Sci. U. S. A. **102:**1472–1477.
65. **Sieczkarski, S. B., and G. R. Whittaker.** 2002. Dissecting virus entry via endocytosis. J. Gen. Virol. **83:**1535–1545.
66. **Simmons, G., A. J. Rennekamp, N. Chai, L. H. Vandenberghe, J. L. Riley, and P. Bates.** 2003. Folate receptor alpha and caveolae are not required for Ebola virus glycoprotein-mediated viral infection. J. Virol. **77:**13433–13438.
67. **Sinn, P. L., J. D. Goreham-Voss, A. C. Arias, M. A. Hickey, W. Maury, C. P. Chikkanna-Gowda, and P. B. McCray, Jr.** 2007. Enhanced gene expression conferred by stepwise modification of a nonprimate lentiviral vector. Hum. Gene Ther. **18:**1244–1252.
68. **Sinn, P. L., M. A. Hickey, P. D. Staber, D. E. Dylla, S. A. Jeffers, B. L. Davidson, D. A. Sanders, and P. B. McCray, Jr.** 2003. Lentivirus vectors pseudotyped with filoviral envelope glycoproteins transduce airway epithelia from the apical surface independently of folate receptor alpha. J. Virol. **77:**5902–5910.
69. **Sullivan, N., Z. Y. Yang, and G. J. Nabel.** 2003. Ebola virus pathogenesis: implications for vaccines and therapies. J. Virol. **77:**9733–9737.
70. **Swanepoel, R., S. B. Smit, P. E. Rollin, P. Formenty, P. A. Leman, A. Kemp, F. J. Burt, A. A. Grobbelaar, J. Croft, D. G. Bausch, H. Zeller, H. Leirs, L. E. Braack, M. L. Libande, S. Zaki, S. T. Nichol, T. G. Ksiazek, and J. T. Paweska.** 2007. Studies of reservoir hosts for Marburg virus. Emerg. Infect. Dis. **13:**1847–1851.
71. **Takada, A., C. Robison, H. Goto, A. Sanchez, K. G. Murti, M. A. Whitt, and Y. Kawaoka.** 1997. A system for functional analysis of Ebola virus glycoprotein. Proc. Natl. Acad. Sci. U. S. A. **94:**14764–14769.
72. **Towner, J. S., B. R. Amman, T. K. Sealy, S. A. Carroll, J. A. Comer, A. Kemp, R. Swanepoel, C. D. Paddock, S. Balinandi, M. L. Khristova, P. B. Formenty, C. G. Albarino, D. M. Miller, Z. D. Reed, J. T. Kayiwa, J. N. Mills, D. L. Cannon, P. W. Greer, E. Byaruhanga, E. C. Farnon, P. Atimnedi, S. Okware, E. Katongole-Mbidde, R. Downing, J. W. Tappero, S. R. Zaki, T. G. Ksiazek, S. T. Nichol, and P. E. Rollin.** 2009. Isolation of genetically diverse Marburg viruses from Egyptian fruit bats. PLoS Pathog. **5:**e1000536.
73. **Towner, J. S., X. Pourrut, C. G. Albarino, C. N. Nkogue, B. H. Bird, G. Grard, T. G. Ksiazek, J. P. Gonzalez, S. T. Nichol, and E. M. Leroy.** 2007. Marburg virus infection detected in a common African bat. PLoS One **2:**e764.
74. **van der Poel, W. H., P. H. Lina, and J. A. Kramps.** 2006. Public health awareness of emerging zoonotic viruses of bats: a European perspective. Vector Borne Zoonotic Dis. **6:**315–324.
75. **Wang, G., V. Slepushkin, J. Zabner, S. Keshavjee, J. C. Johnston, S. L. Sauter, D. J. Jolly, T. W. Dubensky, Jr., B. L. Davidson, and P. B. McCray, Jr.** 1999. Feline immunodeficiency virus vectors persistently transduce nondividing airway epithelia and correct the cystic fibrosis defect. J. Clin. Invest. **104:**R55–R62.
76. **Watanabe, S., A. Takada, T. Watanabe, H. Ito, H. Kida, and Y. Kawaoka.** 2000. Functional importance of the coiled-coil of the Ebola virus glycoprotein. J. Virol. **74:**10194–101201.
77. **Watarai, M., S. Makino, Y. Fujii, K. Okamoto, and T. Shirahata.** 2002. Modulation of Brucella-induced macropinocytosis by lipid rafts mediates intracellular replication. Cell. Microbiol. **4:**341–355.
78. **Will, C., E. Muhlberger, D. Linder, W. Slenczka, H. D. Klenk, and H. Feldmann.** 1993. Marburg virus gene 4 encodes the virion membrane protein, a type I transmembrane glycoprotein. J. Virol. **67:**1203–1210.
79. **Wool-Lewis, R. J., and P. Bates.** 1998. Characterization of Ebola virus entry by using pseudotyped viruses: identification of receptor-deficient cell lines. J. Virol. **72:**3155–3160.
80. **Yang, Z., R. Delgado, L. Xu, R. F. Todd, E. G. Nabel, A. Sanchez, and G. J. Nabel.** 1998. Distinct cellular interactions of secreted and transmembrane Ebola virus glycoproteins. Science **279:**1034–1037.
81. **Yonezawa, A., M. Cavrois, and W. C. Greene.** 2005. Studies of Ebola virus glycoprotein-mediated entry and fusion by using pseudotyped human immunodeficiency virus type 1 virions: involvement of cytoskeletal proteins and enhancement by tumor necrosis factor alpha. J. Virol. **79:**918–926.